Journal of ELECTRONIC MATERIALS, Vol. 46, No. 5, 2017
DOI: 10.1007/s11664-016-4847-0
© 2016 The Minerals, Metals & Materials Society

Synthesis and Thermoelectric Properties of $Ce_{1-z}Pr_zFe_{4-x}Co_xSb_{12}$ Skutterudites

KWON-MIN SONG,[1] DONG-KIL SHIN,[1] KYUNG-WOOK JANG,[2] SOON-MOK CHOI,[3] SOONIL LEE,[4] WON-SEON SEO,[4] and IL-HO KIM[1,5]

1.—Department of Materials Science and Engineering, Korea National University of Transportation, Chungju, Chungbuk 27469, Korea. 2.—Department of Advanced Materials Engineering, Hanseo University, Seosan, Chungnam 31962, Korea. 3.—School of Energy, Materials and Chemical Engineering, Korea University of Technology and Education, Cheonan, Chungnam 31253, Korea. 4.—Energy and Environmental Materials Division, Korea Institute of Ceramic Engineering and Technology, Jinju, Gyeongnam 52851, Korea. 5.—e-mail: ihkim@ut.ac.kr

p-Type $Ce_{1-z}Pr_zFe_{4-x}Co_xSb_{12}$ skutterudites were prepared by encapsulated melting, quenching, annealing, and hot pressing. While the skutterudite phase was successfully synthesized, a small amount of the secondary phase ($FeSb_2$) was observed. According to the scanning electron microscope analysis, $(Ce,Pr)Sb_2$ phases were also observed for Co-substituted specimens ($x = 0.5$). The electrical conductivity decreased with increasing temperature, implying a degenerate semiconductor behavior, and also decreased with increasing Co contents. All specimens showed *p*-type characteristics having positive signs of the Hall coefficient and the Seebeck coefficient. The Seebeck coefficient increased with increasing temperature and reached a maximum value at 823 K. The power factor (PF) increased with decreasing Co content and $Ce_{0.75}Pr_{0.25}Fe_4Sb_{12}$ showed a peak value of PF = 3.2 mW m^{-1} K^{-2} at 823 K. The electronic thermal conductivity decreased with increasing Co contents and the lattice thermal conductivity decreased with decreasing Ce and Co contents at high temperature. The thermal conductivity increased at temperatures above 623 K due to bipolar conduction. The dimensionless figure of merit (ZT) showed a maximum value of ZT = 0.84 at 823 K for $Ce_{0.25}Pr_{0.75}Fe_4Sb_{12}$.

Key words: Thermoelectric, skutterudite, double filling, charge transport

INTRODUCTION

Skutterudites have been widely investigated as promising materials for thermoelectric power generation at temperatures from 500 K to 900 K.[1] Filled skutterudites has the chemical formula RM_4X_{12} (space group Im-3), where R is a filler such as an alkali metal, an alkaline earth metal, or a rare earth metal, M is a transition metal such as Fe, Ru, Os, Co, Rh, or Ir, and X is a pnicogen element such as P, As, or Sb.[2–4]

A skutterudite structure has two large voids per unit cell, and the fillers in the voids play two important roles. First, the fillers donate electrons to the host compound to tune the electrical properties. Second, vibrations of fillers in the voids behave as phonon scattering centers and substantially reduce the lattice thermal conductivity.[5,6] Each filler atom has a specific atomic mass and a unique resonant frequency.[7–10] Thus, double or multiple filling can cause more phonon scattering, resulting in the improvement of thermoelectric performance with lower lattice thermal conductivity.[11–13]

Recently, Shin et al.[14] synthesized Pr/Yb-filled *p*-type skutterudites by hot pressing and reported that filling with different types of atoms could reduce the lattice thermal conductivity due to enhanced phonon scattering. Dahal et al.[4] prepared Ce/Nd-filled *p*-type skutterudites by hot pressing and reported a peak ZT = 1.1 at 748 K for $Ce_{0.4}Nd_{0.4}Fe_{3.7}Ni_{0.3}Sb_{12}$. Liu et al.[15] synthesized Ce/Yb-

(Received May 16, 2016; accepted August 2, 2016; published online August 12, 2016)

filled *p*-type skutterudites by spark plasma sintering and reported a peak ZT = 1.0 at 700 K for $Ce_{0.6}Yb_{0.4}Fe_3CoSb_{12}$. In this study, Ce/Pr-doubled-filled and Co-substituted *p*-type $Ce_{1-z}Pr_zFe_{4-x}Co_xSb_{12}$ skutterudites were prepared, and their charge transport and thermoelectric properties were examined.

EXPERIMENTAL PROCEDURE

$Ce_{1-z}Pr_zFe_{4-x}Co_xSb_{12}$ (z = 0.25, 0.75 and x = 0, 0.25, 0.5) skutterudites were prepared by encapsulated melting and hot pressing. Ce (purity 99.9%, Sigma Aldrich), Pr (purity 99.9%, Kojundo), Fe (purity 99.95%, Cerac), Co (purity 99.95%, Alfa Aesar), and Sb (purity 99.999%, LTS) were melted at 1323 K for 10 h in an evacuated quartz tube coated on the inside with carbon and were then quenched in water. The quenched ingots were annealed at 873 K for 24 h to transform to the skutterudite phase and to homogenize the material. The synthesized ingots were ground to powder having a particle size <75 μm. The powder was hot-pressed in a graphite die with an internal diameter of 10 mm at 898 K under 70 MPa for 1 h in a vacuum.

The phase was analyzed by using an x-ray diffractometer (XRD; Bruker D8 Advance) with Cu K_α radiation in the θ–2θ mode (2θ = 10°–90°). The microstructure was observed by using a scanning electron microscope (SEM; FEI Quanta400) with energy dispersive spectroscopy (EDS; Oxford JSM-5800). The Hall coefficient, carrier concentration, and mobility were measured using the van der Pauw method (Keithley 7065) in a constant magnetic field (1 T) and electric current (50 mA) at room temperature by assuming the parabolic single band. The electrical conductivity and Seebeck coefficient were measured using the four-probe method (Ulvac-Riko ZEM3). Thermal diffusivity was measured using the laser flash method (Ulvac-Riko TC9000H), and the thermal conductivity was then calculated using the equation $\kappa = Dc_pd$, where D is the thermal diffusivity, c_p is the heat capacity at constant pressure, and d is the density of the specimen. Finally, the power factor (PF) and the dimensionless figure of merit (ZT) were evaluated at temperatures ranging from 323 K to 823 K. The errors in each measurement were <5%, and the overall uncertainty on the ZT value was estimated as 20%.

RESULTS AND DISCUSSION

Figure 1 presents the XRD patterns of $Ce_{1-z}Pr_zFe_{4-x}Co_xSb_{12}$ skutterudites. All specimens were successfully synthesized to the skutterudite phase of the International Center for Diffraction Data (ICDD PDF# 56-1091), although a small amount of the marcasite phase ($FeSb_2$) was identified. However, the peak intensity of the marcasite phase decreased with increasing Co content, as shown in Fig. 1b and c. These results indicated that the Fe-Sb-based skutterudite phase was stabilized by void filling and charge compensation. The diffraction peaks shifted to higher angles with increasing Co content, which implies a decrease in the lattice constant. The lattice constant decreased from 0.9125 to 0.9110 nm with increasing Co content, as shown in Table I.

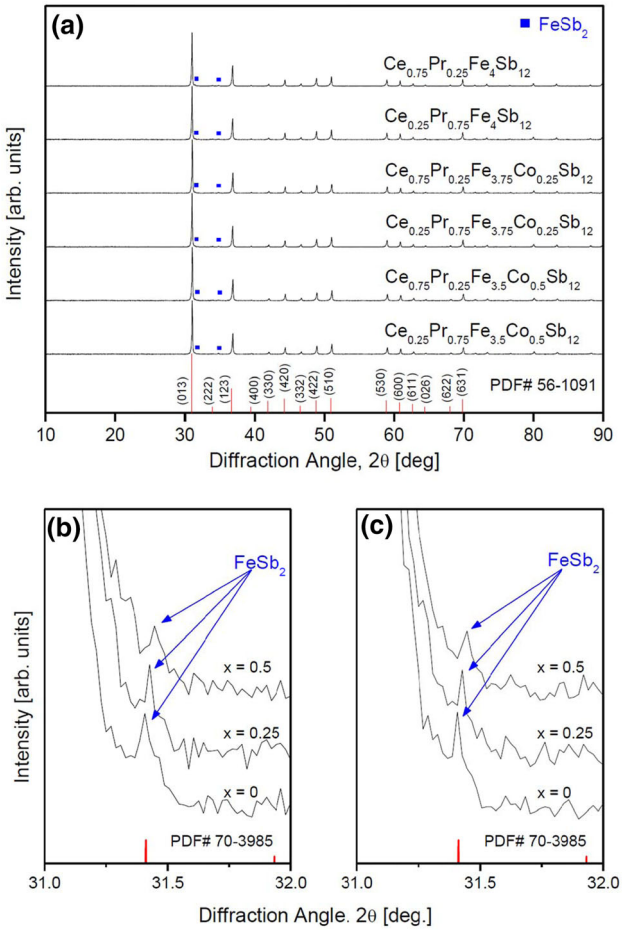

Fig. 1. XRD patterns of (a) $Ce_{1-z}Pr_zFe_{4-x}Co_xSb_{12}$ skutterudites and expanded XRD patterns of the specimens with (b) z = 0.25 and (c) z = 0.75.

Figure 2 shows the SEM images and the EDS analysis data for $Ce_{1-z}Pr_zFe_{4-x}Co_xSb_{12}$. All specimens had relative densities of higher than 97% compared with the theoretical density. The main phase was the skutterudite (regions A, C, E, G, I, and L) and the secondary phase was $FeSb_2$ (regions B, D, F, H, J, and M), which was in good agreement with the XRD results in Fig. 1. However, a small number of $(Ce,Pr)Sb_2$ phases (regions K and N) were also observed in the Co-substituted specimens (x = 0.5), as shown in Fig. 2e and f. The formation of $(Ce,Pr)Sb_2$ was expected due to the filling fraction limit. The $(Ce,Pr)Sb_2$ phases were not detected in the XRD analysis because their amounts were too small to detect. The actual compositions of all specimens were similar to their nominal

Table I. Relative density, lattice constant, and charge transport properties of $Ce_{1-z}Pr_zFe_{4-x}Co_xSb_{12}$ at room temperature

Composition		Relative density (%)	Lattice constant (nm)	Hall coefficient (10^{-3} cm^3 C^{-1})	Carrier mobility (cm^2 V^{-1} s^{-1})	Carrier concentration (10^{21} cm^{-3})
Nominal	**Actual**					
$Ce_{0.75}Pr_{0.25}Fe_4Sb_{12}$	$Ce_{0.72}Pr_{0.23}Fe_4Sb_{11.77}$	98.91	0.9125	2.13	4.54	2.94
$Ce_{0.25}Pr_{0.75}Fe_4Sb_{12}$	$Ce_{0.23}Pr_{0.70}Fe_4Sb_{11.65}$	98.93	0.9124	2.32	4.83	2.70
$Ce_{0.75}Pr_{0.25}Fe_{3.75}Co_{0.25}Sb_{12}$	$Ce_{0.71}Pr_{0.22}Fe_{3.73}Co_{0.27}Sb_{11.78}$	98.86	0.9117	3.40	6.46	1.84
$Ce_{0.25}Pr_{0.75}Fe_{3.75}Co_{0.25}Sb_{12}$	$Ce_{0.22}Pr_{0.68}Fe_{3.67}Co_{0.33}Sb_{11.48}$	98.83	0.9116	3.44	6.37	1.82
$Ce_{0.75}Pr_{0.25}Fe_{3.5}Co_{0.5}Sb_{12}$	$Ce_{0.67}Pr_{0.22}Fe_{3.45}Co_{0.55}Sb_{11.50}$	98.87	0.9111	4.44	7.04	1.41
$Ce_{0.25}Pr_{0.75}Fe_{3.5}Co_{0.5}Sb_{12}$	$Ce_{0.20}Pr_{0.68}Fe_{3.46}Co_{0.54}Sb_{11.55}$	98.79	0.9110	4.61	7.31	1.35

compositions, as shown in Table I. However, the number of fillers (Ce/Pr) was slightly lower than nominal compositions, which were expected due to the filling fraction limit (FFL) and the volatilization during the preparation process. The filling fraction decreased with increasing Co content at actual compositions. The FFL in the Ce-filled skutterudites decreases with increasing Co content.[16–19] Therefore, the charge compensation (Co substitution) had required the partial double filling of Ce/Pr, where the total filling content of two fillers is lower than unity.

Table I summarizes the charge transport properties of $Ce_{1-z}Pr_zFe_{4-x}Co_xSb_{12}$ at room temperature. The Hall coefficients of all specimens have positive values, indicating *p*-type conductions by major carriers of holes. The carrier concentration decreased with increasing Co contents. The carrier concentration ranged from 1.35×10^{21} cm^{-3} to 2.94×10^{21} cm^{-3} with (Ce/Pr) filling ratio and Co substitution content.

Figure 3 presents the temperature dependence of the electrical conductivity for $Ce_{1-z}Pr_zFe_{4-x}Co_xSb_{12}$. The electrical conductivity decreased with increasing temperature, showing that all specimens were degenerate semiconductors. The electrical conductivity decreased with increasing Co contents due to the decrease in the carrier concentration, as shown in Table I. The electrical conductivity had maximum values of 2.13×10^5 Sm^{-1} to 1.44×10^5 Sm^{-1} at temperatures ranging from 323 K to 823 K for $Ce_{0.75}Pr_{0.25}Fe_4Sb_{12}$ and minimum values ranging from 1.61×10^5 Sm^{-1} to 1.04×10^5 Sm^{-1} at temperatures ranging from 323 K to 823 K for $Ce_{0.25}Pr_{0.75}Fe_{3.5}Co_{0.5}Sb_{12}$.

Figure 4 shows the temperature dependence of the Seebeck coefficient for $Ce_{1-z}Pr_zFe_{4-x}Co_xSb_{12}$. The Seebeck coefficients of all specimens had positive signs of *p*-type conductions, and increased with increasing temperature to peak values at 823 K. Park et al.[20] reported the Seebeck coefficient of 145 μVK^{-1} at 823 K for $CeFe_4Sb_{12}$. In this study, the Seebeck coefficient reached 151 μVK^{-1} at 823 K for $Ce_{0.25}Pr_{0.75}Fe_4Sb_{12}$. The Seebeck coefficient also increased with increasing Co content because the carrier concentration decreased with increasing Co content. The Seebeck coefficient of a *p*-type semiconductor can be expressed as $\alpha = (8/3)\pi^2 k_B^2 m^* Te^{-1}h^{-2}(\pi/3n)^{2/3}$, where k_B, e, h, m^*, and n represent the Boltzmann constant, the electronic charge, the Planck constant, the effective carrier mass, and the carrier concentration, respectively.[21] Therefore, the Seebeck coefficient increases with decreasing carrier concentration and increases with increasing temperature, while it decreases with the increased carrier concentration caused by intrinsic transition at high temperatures. On the other hand, the Seebeck coefficient is also affected by carrier scattering with varying of microstructure. In this study, the alteration of Seebeck coefficients may be affected by the carrier concentration and secondary phases.

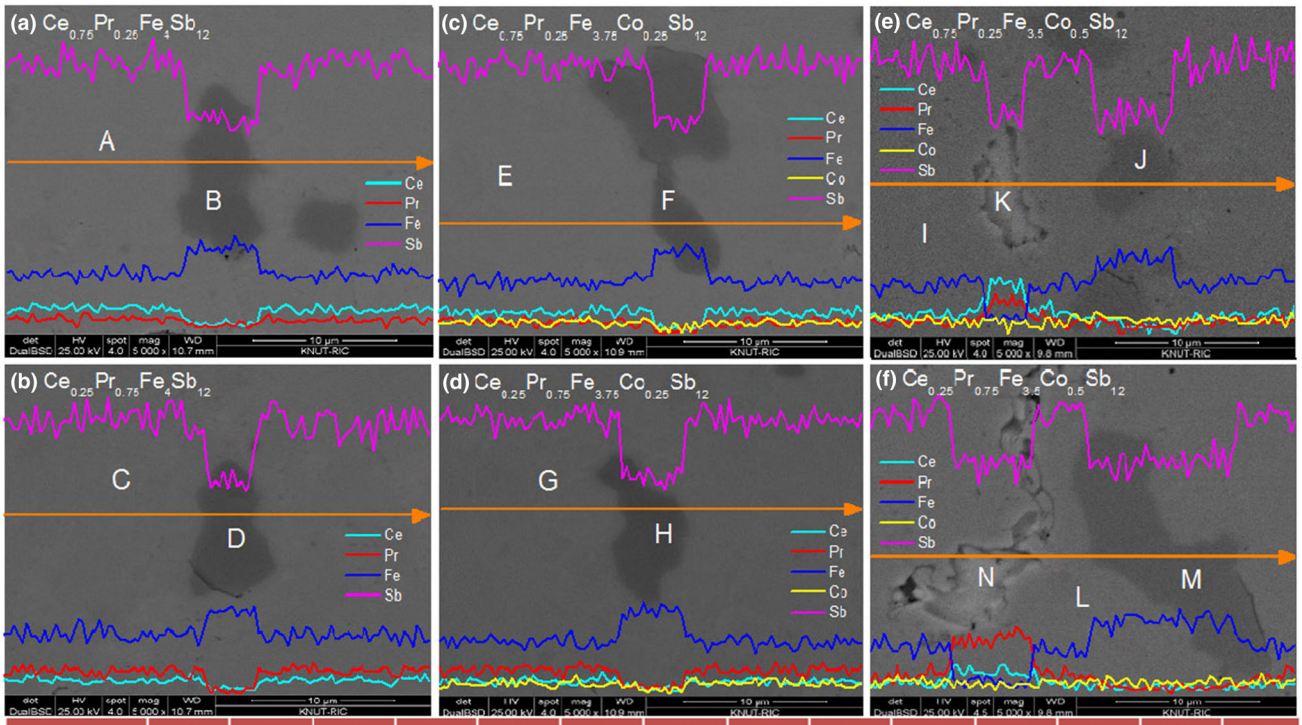

Region	A	B	C	D	E	F	G	H	I	J	K	L	M	N
Ce (at.%)	3.97	0.22	1.38	0.13	3.79	0.20	1.41	0.11	3.68	0.11	20.18	1.24	0.02	7.62
Pr (at.%)	1.45	0.18	3.95	0.19	1.48	0.16	3.79	0.13	1.36	0.10	8.89	3.54	0.09	19.83
Fe (at.%)	21.93	30.44	21.69	31.45	21.01	30.10	21.98	32.08	18.72	28.68	1.08	19.11	27.95	1.12
Co (at.%)	-	-	-	-	1.40	0.19	1.43	0.30	2.43	0.92	0.57	2.04	1.79	0.19
Sb (at.%)	73.55	69.16	72.98	68.23	72.32	69.37	71.39	67.38	73.80	70.19	69.28	74.07	70.15	71.81

Fig. 2. SEM images, EDS line scans, and elemental analysis data of $Ce_{1-z}Pr_zFe_{4-x}Co_xSb_{12}$: (a) $Ce_{0.75}Pr_{0.25}Fe_4Sb_{12}$, (b) $Ce_{0.25}Pr_{0.75}Fe_4Sb_{12}$, (c) $Ce_{0.75}Pr_{0.25}Fe_{3.75}Co_{0.25}Sb_{12}$, (d) $Ce_{0.25}Pr_{0.75}Fe_{3.75}Co_{0.25}Sb_{12}$, (e) $Ce_{0.75}Pr_{0.25}Fe_{3.5}Co_{0.5}Sb_{12}$, and (f) $Ce_{0.25}Pr_{0.75}Fe_{3.5}Co_{0.5}Sb_{12}$.

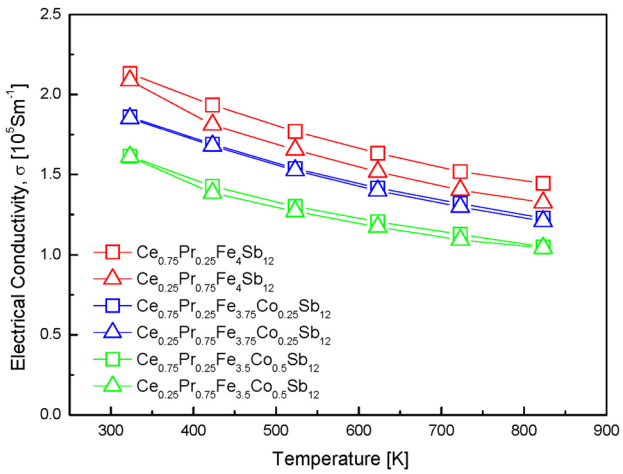

Fig. 3. Temperature dependence of the electrical conductivity for $Ce_{1-z}Pr_zFe_{4-x}Co_xSb_{12}$.

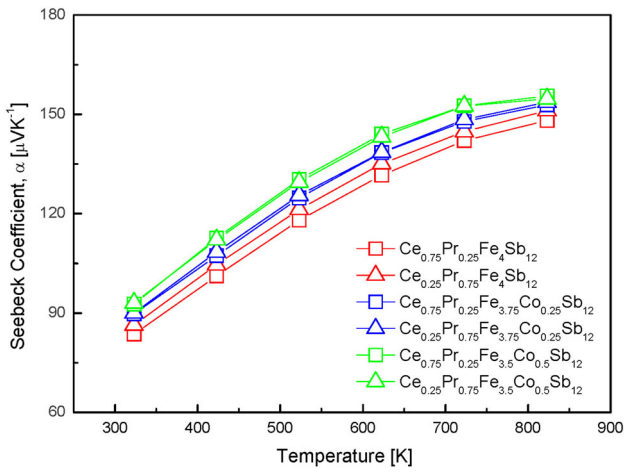

Fig. 4. Temperature dependence of the Seebeck coefficient for $Ce_{1-z}Pr_zFe_{4-x}Co_xSb_{12}$.

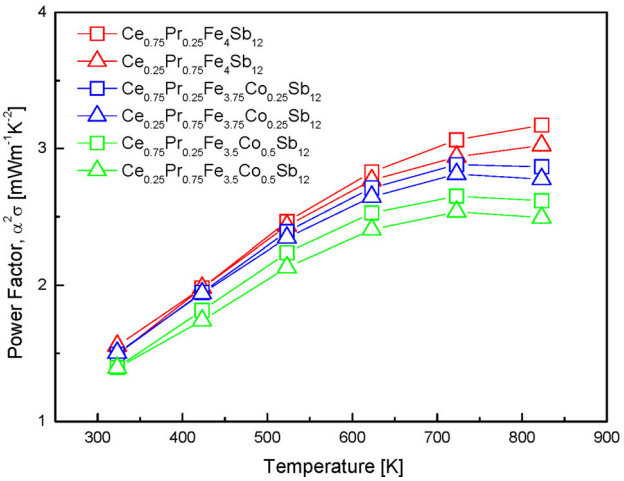

Fig. 5. Temperature dependence of the power factor for $Ce_{1-z}Pr_z Fe_{4-x}Co_xSb_{12}$.

Figure 5 presents the temperature dependence of the power factor (PF) for $Ce_{1-z}Pr_zFe_{4-x}Co_xSb_{12}$. The PF values increased with increasing temperature and reached peak values at 723 K for Co-substituted specimens. The PF values increased with decreasing Co content because the electrical conductivity increased with increasing carrier concentration. The PF values also increased with increasing Ce content because the electrical conductivity slightly increased with increasing Ce content while the Seebeck coefficients were similar. Park et al.[20] reported the PF = 2.7 mW m^{-1} K^{-2} at 823 K for $CeFe_4Sb_{12}$. In this study, the PF = 3.0 mW m^{-1} K^{-2} was obtained at 823 K for $Ce_{0.25}Pr_{0.75}Fe_4Sb_{12}$ and the maximum PF = 3.2 mW m^{-1} K^{-2} was attained at 823 K for $Ce_{0.75}Pr_{0.25}Fe_4Sb_{12}$.

Figure 6 shows the temperature dependence of the thermal conductivity for $Ce_{1-z}Pr_zFe_{4-x}Co_xSb_{12}$. The thermal conductivity decreased with increasing Pr and Co contents, as shown in Fig. 6a. The thermal conductivity of all specimens also increased due to bipolar conduction at temperatures above 723 K and ranged from 2.4 Wm^{-1} K^{-1} to 3.1 Wm^{-1} K^{-1} at temperatures ranging from 323 K to 823 K. The thermal conductivity (κ) is the sum of the lattice thermal conductivity (κ_L) and the electronic thermal conductivity (κ_E), which can be separated by using the Wiedemann–Franz law ($\kappa_E = L\sigma T$), where L is the Lorenz constant, which was assumed as $L = 2.0 \times 10^{-8}$ V^2 K^{-2} in this study.[22] As shown in Fig. 6b, the lattice conductivity was not varied with the filling ratios of Ce and Pr.

The lattice thermal resistivity $\left(W_L = \kappa_L^{-1}\right)$ of the filled skutterudite was expressed as $W_L = W_M + W_{PD} + W_R \approx (r_{cage} - r_{ion})$, where W_M is the thermal resistivity of the unfilled skutterudite, W_{PD} is the thermal resistivity contributed by point defects, W_R is the thermal resistivity contributed by

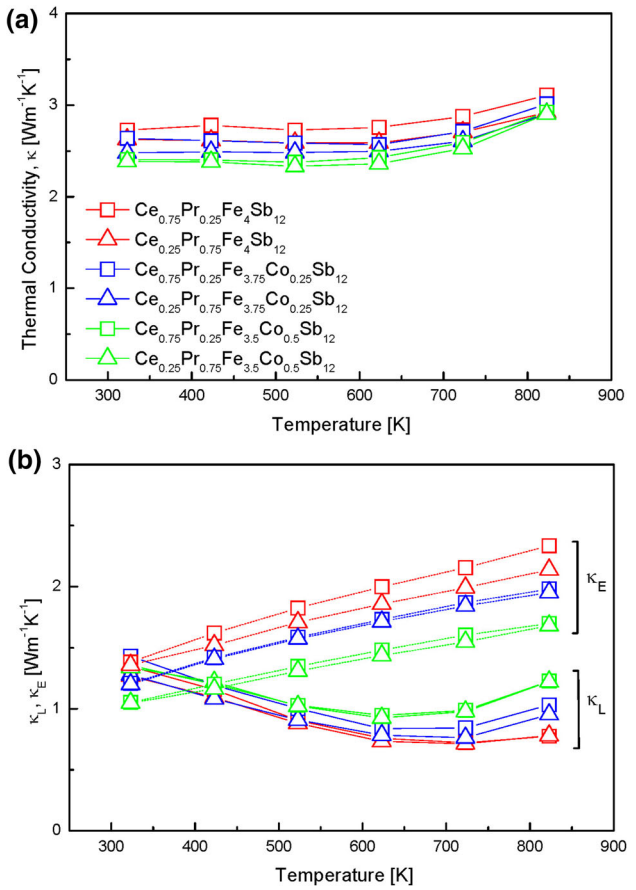

Fig. 6. Temperature dependence of (a) thermal conductivity and (b) the lattice and electronic thermal conductivities for $Ce_{1-z}Pr_z Fe_{4-x}Co_xSb_{12}$.

resonant scattering, r_{cage} is the void radius (0.1892 nm), and r_{ion} is the ionic radius of a filler.[23] Therefore, the lattice conductivity decreases if a filler with a small ionic radius is used. In this study, the ionic radii of Ce and Pr were 0.134 and 0.133 nm, respectively.[22] Therefore, the lattice conductivity can be similar to the filling ratio of the Ce and Pr contents. The electronic thermal conductivity decreased with increasing Pr and Co contents due to the decrease in the carrier concentration.

Figure 7 presents the temperature dependence of the dimensionless figure of merit (ZT) for $Ce_{1-z}Pr_z Fe_{4-x}Co_xSb_{12}$. The ZT values increased with increasing temperature and the Co-substituted (x = 0.5) specimens showed peak values at 723 K. Although the differences in ZT values were little at low temperatures, their differences became larger at high temperatures. Co substitution had influence on the ZT values due to the change in the onset temperature of intrinsic conduction, which moved to lower temperatures with increasing Co content. Although the PF values of the specimens with x = 0 or 0.25 decreased with increasing Pr content, the ZT values increased because the thermal conductivity decreased with increasing Pr content.

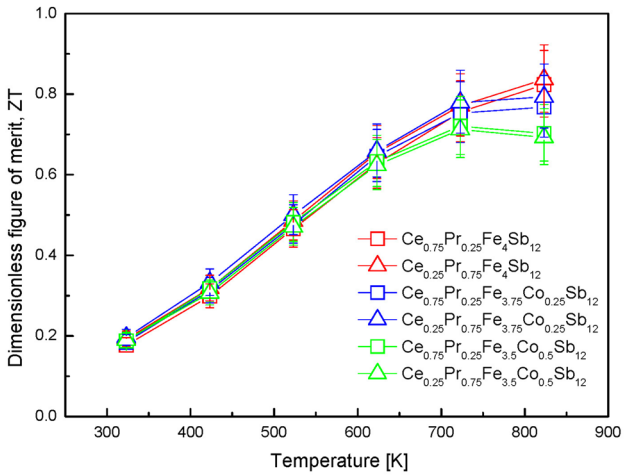

Fig. 7. Temperature dependence of the dimensionless figure of merit for $Ce_{1-z}Pr_zFe_{4-x}Co_xSb_{12}$.

Consequently, the maximum value of $ZT_{max} = 0.84$ was obtained at 823 K for $Ce_{0.25}Pr_{0.75}Fe_4Sb_{12}$. Park et al.[20] reported the $ZT_{max} = 0.75$ at 823 K for $CeFe_4Sb_{12}$ and Shin et al.[24] reported the $ZT_{max} = 0.79$ at 823 K for $PrFe_4Sb_{12}$. In this study, Ce/Pr double filling could increase the ZT value. However, the ZT value decreased with increasing Co content, while it was expected that thermoelectric performance could be improved by partial double filling of Ce and Pr, where the total filling content of two fillers is lower than unity.

CONCLUSION

$Ce_{1-z}Pr_zFe_{4-x}Co_xSb_{12}$ ($z = 0.25$, 0.75 and $x = 0$, 0.25, 0.5) skutterudites were prepared by a melting—quenching—annealing—hot pressing process. While the major phase was the skutterudite, a small amount of $FeSb_2$ phase was produced. $(Ce/Pr)Sb_2$ phases were also observed for Co-substituted specimens with $x = 0.5$. The Hall coefficients and the Seebeck coefficients of all specimens showed positive signs, indicating that all specimens behaved as *p*-type characteristics. The electrical conductivity decreased with increasing temperature similar to degenerate semiconductors. The electrical conductivity also decreased with increasing Co contents because the carrier concentration decreased. The PF showed peak values at temperatures between 723 K and 823 K. The thermal conductivity decreased with increasing Pr content because the lattice and the electronic thermal conductivities decreased. The lattice thermal conductivity decreased with increasing Pr content, meaning that Pr contributed more than Ce to decreasing the lattice thermal conductivity. The maximum value of $ZT_{max} = 0.84$ was obtained at 823 K for $Ce_{0.25}Pr_{0.75}Fe_4Sb_{12}$, while $ZT_{max} = 0.79$ was achieved at 823 K for $Ce_{0.25}Pr_{0.75}Fe_{3.75}Co_{0.25}Sb_{12}$.

ACKNOWLEDGEMENTS

This study was supported by the Dual Use Technology Program of the Agency for Defense Development, Republic of Korea.

REFERENCES

1. L.E. Bell, *Science* 321, 1457 (2008).
2. A. Leithe-Jasper, W. Schnelle, H. Rosner, A. Rabis, M. Baenitz, A.A. Gippius, E.N. Morozova, J.A. Mydosh, and Y. Grin, *Phys. Rev. Lett.* 91, 037208 (2013).
3. D.R. Thompson, C. Liu, J. Yang, J.R. Salvador, D.B. Haddad, N.D. Ellison, R.A. Waldo, and J. Yang, *Acta Mater.* 92, 152 (2015).
4. T. Dahal, Q. Jie, Y. Lan, C. Guo, and Z. Ren, *Phys. Chem. Chem. Phys.* 16, 18170 (2014).
5. B.C. Scales, D. Mandrus, and R.K. Williams, *Science* 22, 1325 (1996).
6. D.J. Singh and M.H. Du, *Phys. Rev. B* 82, 075115 (2010).
7. M.V. Keepens, D. Mandrus, B.C. Sales, B.C. Chakoumakos, P. Day, R. Coldea, B. Maple, D.A. Gajewski, E.J. Freeman, and S. Bennington, *Nature* 395, 876 (1998).
8. L. Zhang, A. Grytsiv, P. Rogl, E. Bauer, and M. Zehebauer, *J. Phys. D* 42, 225405 (2009).
9. J. Yang, W. Zhang, Z.Q. Bai, Z. Mei, and L.D. Chen, *Appl. Phys. Lett.* 90, 192111 (2007).
10. X.F. Tang, Q. Zhang, L.D. Chen, T. Goto, and T. Hirai, *J. Appl. Phys.* 97, 093712 (2005).
11. X. Shi, J.O. Yang, J.R. Salvador, M.F. Chi, J.Y. Cho, H. Wang, S.Q. Bai, J.H. Wang, W.Q. Zhang, and L.D. Chen, *J. Am. Chem. Soc.* 133, 7837 (2011).
12. X. Shi, H. Kong, C.P. Li, C. Uher, J. Yang, J.R. Salvador, H. Wang, L. Chen, and W. Zhang, *Appl. Phys. Lett.* 92, 182101 (2008).
13. W. Zhao, P. Wei, Q. Zhang, C. Dong, L. Liu, and X.F. Tang, *J. Am. Chem. Soc.* 131, 3713 (2009).
14. D.K. Shin and I.H. Kim, *J. Korean Phys. Soc.* 67, 1208 (2015).
15. R. Liu, J. Yang, X. Chen, X. Shi, L. Chen, and C. Uher, *Intermetallics* 19, 1747 (2011).
16. G.P. Meisner, D.T. Morelli, S. Hu, J. Yang, and C. Uher, *Phys. Rev. Lett.* 80, 3551 (1998).
17. D. Bérardan, C. Godart, E. Alleno, E. Leroy, and P. Rogl, *J. Alloys Compd.* 350, 30 (2003).
18. H. Kitagawa, M. Hasaka, T. Morimura, H. Nakashima, and S. Kondo, *Mater. Res. Bull.* 35, 185 (2000).
19. X.F. Tang, L.D. Chen, T. Goto, T. Hirai, and R.Z. Yuan, *J. Mater. Sci.* 36, 5435 (2001).
20. K.H. Park, S.I. Lee, W.S. Seo, D.K. Shin, and I.H. Kim, *J. Korean Phys. Soc.* 64, 863 (2014).
21. Y.C. Lan, A.J. Minnich, G. Chen, and Z.F. Ren, *Adv. Funct. Mater.* 20, 357 (2010).
22. C. Kittel, *Introduction to Solid State Physics*, 6th ed. (New York: Wiley, 1986), p. 152.
23. P.F. Qui, J. Yang, R.H. Liu, X. Shi, X.Y. Huang, G.J. Snyder, W. Zhang, and L.D. Chen, *J. Appl. Phys.* 109, 063713 (2011).
24. D.K. Shin and I.H. Kim, *J. Korean Phys. Soc.* 65, 2071 (2014).